Effects of buried high-Z layers on fast electron propagation

Yang, X., Xu, H., Zhuo, H., Ma, Y., Shao, F., Yin, Y., & Borghesi, M. (2014). Effects of buried high-Z layers on fast electron propagation. DOI: 10.1140/epjd/e2013-40576-4

Published in:
The European Physical Journal D - Atomic, Molecular, Optical and Plasma Physics

Document Version:
Publisher's PDF, also known as Version of record

Eur. Phys. J. D (2014) 68: 30
DOI: 10.1140/epjd/e2013-40576-4

THE EUROPEAN PHYSICAL JOURNAL D

Regular Article

Effects of buried high-Z layers on fast electron propagation

Xiaohu Yang[1], Han Xu[2], Hongbin Zhuo[1], Yanyun Ma[1], Fuqiu Shao[1], Yan Yin[2], and Marco Borghesi[3,4,a]

[1] College of Science, National University of Defense Technology, Changsha 410073, P.R. China
[2] State Key Lab of High Performance Computing, National University of Defense Technology, Changsha 410073, P.R. China
[3] School of Mathematics and Physics, Queen's University of Belfast, Belfast BT7 1NN, UK
[4] Institute of Physics of the ASCR, ELI-Beamlines project, Na Slovance 2, 18221 Prague, Czech Republic

Received 17 September 2013 / Received in final form 6 November 2013
Published online 13 February 2014 –

Abstract. By extending a prior model [A.R. Bell, J.R. Davies, S.M. Guerin, Phys. Rev. E **58**, 2471 (1998)], the magnetic field generated during the transport of a fast electron beam driven by an ultraintense laser in a solid target is derived analytically and applied to estimate the effect of such field on fast electron propagation through a buried high-Z layer in a lower-Z target. It is found that the effect gets weaker with the increase of the depth of the buried layer, the divergence of the fast electrons, and the laser intensity, indicating that magnetic field effects on the fast electron divergence as measured from K_a X-ray emission may need to be considered for moderate laser intensities. On the basis of the calculations, some considerations are made on how one can mitigate the effect of the magnetic field generated at the interface.

1 Introduction

The transport through high density plasmas of relativistic electron beams generated by ultraintense laser-plasma interaction has attracted significant recent interest [1–5] because of their potential application in ultrashort bright X-ray sources [6,7], laser-driven ion acceleration [8], and the fast ignitor scheme for inertial confinement fusion [9]. An accurate characterization of the fast electron properties is of particular importance for these applications.

The divergence of the fast electron beams is one of the critical parameters, affecting the beam current density and the energy deposition in an ICF target. Various diagnostic methods have been used to measure the fast electron divergence, such as K_a X-ray emission [10], shadowgraphy [11], optical self-emission from the rear surface [12], and proton emission [13]. It is generally found that the divergence measured in the experiments increases with laser intensity [14], though some discrepancy exists among the different diagnostic methods because each one is dependent on different parameters [11]. It should also be noted that the divergence investigated in the experiments usually results from the transport effects of the electrons in the target. Recently, Yang et al. [15] proposed a scheme to infer the intrinsic divergence of the fast electron beam by K_a X-ray emission with the help of an external axial magnetic field; the intrinsic divergence where can be inferred from measurements of the beam radius at different depths under the effect of an appropriate external axial magnetic field.

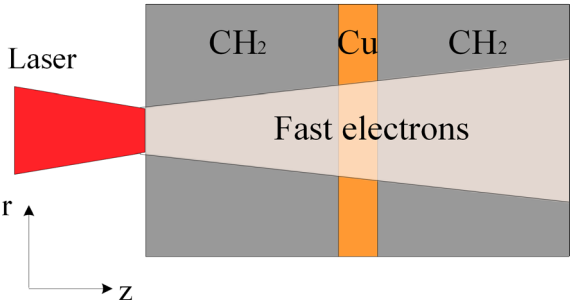

Fig. 1. Schematic describing of the target with a buried high-Z tracer layer.

A high-Z layer (such as Cu, Ti) is usually buried in a low-Z target (such as CH_2, Al) to infer the fast electron divergence in the K_a X-ray emission scheme, as shown in Figure 1. X-rays are emitted via electron-impact ionization of the innermost shell and subsequent fluorescence, in energy ranges from several keV to several tens keV for high-Z materials. However, Bell et al. [16] showed that a strong self-generated magnetic field is generated at the interface between materials with different resistivities, which can magnetize the fast electrons crossing such interface, resulting in an inhibition of fast electron propagation in the target. Evans [17] observed strong magnetic field (∼2500 T) generated at the interface between an Al layer and a CH substrate using LSP simulations, causing the fast electrons to propagate along the interface. Wei et al. [18] observed that the maximum energy and number of energetic protons from double-layer targets are greatly reduced in comparison to pure aluminum and

[a] e-mail: m.borghesi@qub.ac.uk

plastic targets of the same thickness, and attributed this effect to strong magnetic field generation at the interface. Furthermore, Gizzi et al. [19] also found that the laser-driven ion beam was emitted with a much smaller angular spread from a metal foil coated with a dielectric lacquer, compared with the beam from an uncoated metal foil. They also attribute this effect to the growth of the self-generated magnetic field at the metal-dielectric interface, which allows only the higher energy fast electrons propagating close to the axis to leak through the target. All these papers indicate that, the intrinsic divergence of the fast electron beams may be altered by the magnetic field at the surfaces of a buried layer, and that any divergence measurement based on K_a X-ray emission from buried layers should take this effect into account.

In this paper, we revisit the calculations by Bell et al. [16], extending them to the case of a layer embedded in the bulk of the target, and investigating the effect of the B-field at the interface as a function of a range of parameters not explicitly investigated in reference [16]. The magnetic field generated during the fast electron beam transport through a solid target is derived, on the assumption that the fast electron current is neutralized completely by a cold return current. The effect of the magnetic field generated at the buried layer surfaces on the fast electron is estimated through the magnetization of the fast electron beam, as done in reference [16]. It is found that the magnetization becomes weaker with the increase of the depth of the buried layer, the divergence of the fast electrons, and the laser intensity. This confirms that care should be taken when inferring the fast electron divergence measured from the K_a X-ray emission, particularly in case of moderate laser intensities as the measurements may reveal divergence values larger than the intrinsic divergence of the beam.

2 Source of magnetic field generation

We consider an ultraintense laser pulse interacting with a solid target containing a buried high-Z tracer layer. The interaction drives through the target a fast electron beam having a current which greatly exceeds the Alfvén limit [20], as shown in Figure 1. In order to be able to propagate through the target, the fast electron current needs to be neutralized by a return current. For the purpose of estimating the magnetic field at the interface, we assume in first approximation that the fast electrons are unaffected by the magnetic field. With a two-fluid theory, the equation of motion of the nonrelativistic background cold electrons is given by [21]:

$$\frac{\partial \mathbf{v}_e}{\partial t} + (\mathbf{v}_e \nabla)\mathbf{v}_e = -\frac{e}{m_e}(\mathbf{E} + \mathbf{v}_e \times \mathbf{B}) - \frac{\nabla p}{m_e n_e} - \nu_{ei}\mathbf{v}_e, \quad (1)$$

where $\mathbf{v}_e$ is the electron velocity, e is the electron charge, n_e is the electron number density, m_e is the electron mass, $\mathbf{E}$ is the electric field, $\mathbf{B}$ is the magnetic field, $p = n_e k_B T_e$ is the electron thermal pressure, k_B is the Boltzmann constant, T_e is the electron temperature, ν_{ei} is collision frequency of electrons and ions. For an ultraintense laser pulse interacting with a solid target, the electron-ion collision frequency becomes comparable to the local plasma frequency, and the fast electron density is negligible compared to the cold plasma density. In this case, one can neglect the electron inertial term in equation (1) [22],

$$0 = \mathbf{E} + \mathbf{v}_e \times \mathbf{B} + \frac{\nabla p}{e n_e} + e n_e \mathbf{v}_e \eta. \quad (2)$$

The electron-ion collision frequency has been replaced by the resistivity through the expression $\eta = m_e \nu_{ei}/n_e e^2$ in equation (2). Assuming that the fast electron currents can be neutralized completely by the cold return current (i.e., $\mathbf{j}_c = -\mathbf{j}_h$), which is usually satisfied in the situation of ultraintense laser-driven fast electron propagation in high density plasma [23,24], where $\mathbf{j}_c = -e n_e \mathbf{v}_e$ is the cold electron current and $\mathbf{j}_h$ is the fast electron current, one can write

$$\mathbf{E} = -\frac{1}{n_e e}\mathbf{j}_h \times \mathbf{B} - \frac{\nabla p}{e n_e} - \eta \mathbf{j}_h. \quad (3)$$

Taking the curl of equation (3) and combining with Maxwell equations, one can obtain

$$\frac{\partial \mathbf{B}}{\partial t} = \frac{1}{e}\nabla \times \left(\frac{\mathbf{j}_h}{n_e} \times \mathbf{B}\right) + \frac{k_B}{n_e e}\nabla T_e \times \nabla n_e + \nabla \times (\eta \mathbf{j}_h). \quad (4)$$

This expression suggests that a strong magnetic field may be generated as fast electron beams propagate through a steep density or resistivity gradient, which can reflect or trap the fast electrons – this is exactly in the situation taking place in the case of fast electron diagnosis with a high-Z tracer layer. Three terms contribute to the generation of the magnetic field: magnetic force term, thermoelectric source term, and the resistive term, which, respectively, are often dominant in the cases of ideal Magnetohydrodynamics (MHD), long pulse laser-plasma interaction and charged particles transport in a dense background plasma [25,26]. We will show in the following considerations that the resistive magnetic field is dominant for the generation of the magnetic field at the tracer layer surfaces. Note that the effect of the magnetic diffusion is neglected here. The characteristic diffusion distance by the end of the laser pulse can be given by $L_d = (\eta \tau_L/\mu_0)^{1/2}$ [16,24], where τ_L is the duration of the laser pulse. Applying the standard value of the Spitzer resistivity [27] to estimate L_d, one can find that L_d is small for the materials that have been heated and ionized by pecosecond laser pulses [16,24].

For a solid target, background plasma heating by the fast electron beams is mainly via Ohmic heating [28,29], and thus the cold electron temperature can be given by

$$\frac{3}{2} n_e k_B \frac{\partial T_e}{\partial t} = \eta j_c^2 = \eta j_h^2. \quad (5)$$

The Spitzer resistivity is valid for all materials at temperatures higher than 100 eV [27], and is therefore used in this paper:

$$\eta = 10^{-4}\frac{Z \ln \Lambda}{T_e^{3/2}}, \quad (6)$$

where Z is the ionization state of the target and $\ln \Lambda$ is the Coulomb logarithm. One can obtain the temperature T_e by integrating equation (5) directly,

$$T_e = \left(T_0^{5/2} + \frac{3}{5} \times 10^{-4} \frac{Z \ln \Lambda}{n_e k_B} j_h^2 t \right)^{2/5}, \quad (7)$$

where T_0 is the initial temperature of the target.

In the following study, we will use a rigid beam model for the fast electron current [30] to investigate the effect of the self-generated magnetic field at the interface on the fast electron propagation, supposing the fast electron current has an axial symmetry,

$$\mathbf{j}_h = -j_0 \exp(-r^2/r_b^2)\mathbf{e}_z, \quad (8)$$

where $j_0 = \alpha I/T_h$ [23], α is the laser-fast-electron energy conversion efficiency, I is the laser intensity, r_b is the spot radius of the laser pulse, $\mathbf{e}_z$ is the unit vector in the z direction, and T_h is the fast electron temperature given by the ponderomotive scaling [31], i.e.,

$$T_h = m_e c^2 \left(\sqrt{1 + I\lambda^2/(1.37 \times 10^{18}\ \mathrm{W/cm^2})} - 1 \right),$$

where λ is the laser wavelength. Such model was usually applied in the previous hybrid PIC/fluid simulations [28,32,33], where fast electrons are injected into the target at a random angle to the axis with a uniform distribution in an initially specified divergence angle.

3 Results

We firstly consider the situation of a Cu layer buried in a CH_2 target with a buried depth of 25 μm. The thickness of the Cu layer is 5 μm. The materials are blended slightly ($\sim$1 μm) at the interface for numerical reasons. The density and ionization state of the target and tracer layer are given as

$$\begin{aligned} n_e &= \frac{1}{2}(n_{\mathrm{Cu}} - n_{\mathrm{CH}}) \\ &\quad \times \left[\tanh\left(\frac{z-25}{0.2} \right) + \tanh\left(\frac{30-z}{0.2} \right) \right] + n_{\mathrm{CH}}, \\ Z &= \frac{1}{2}(Z_{\mathrm{Cu}} - Z_{\mathrm{CH}}) \\ &\quad \times \left[\tanh\left(\frac{z-25}{0.2} \right) + \tanh\left(\frac{30-z}{0.2} \right) \right] + Z_{\mathrm{CH}}, \end{aligned} \quad (9)$$

where $n_{\mathrm{Cu}} = 2.44 \times 10^{24}/\mathrm{cm^3}$ and $n_{\mathrm{CH}} = 1.14 \times 10^{23}/\mathrm{cm^3}$ are the electron number density of Cu and CH_2, $Z_{\mathrm{Cu}} = 29$ and $Z_{\mathrm{CH}} = 2.67$ are the ionization state of Cu and CH_2, respectively, z is in units of μm. The initial temperature of the target is set to 100 eV. The fast electrons are produced by a laser pulse with an intensity of 10^{19} W/cm^2 and a pulse duration of 0.5 ps. The spot radius of the laser pulse is 10 μm. The fast electron absorption efficiency is set to 0.2 [34,35], thus a fast electron current density of 2.1×10^{12} A/cm^2 is produced. The divergence of the fast electrons is set to 30°. Combining equations (4) and (5), we can obtain the self-generated magnetic field as the fast electrons propagate in the target described by equation (9). For simplicity, a beam profile of

$$\mathbf{j}_h = -j_0 \frac{r_b^2}{(r_b + z\tan(\theta))^2} \exp\left(-\frac{r^2}{(r_b + z\tan(\theta))^2} \right) \mathbf{e}_z$$

is applied for the fast electron current as the fast electron divergence is considered, where θ is the fast electron divergence, z is the distance along the propagation axis from the source. It is based on the fact that the current is conserved during the fast electron propagation. Here we have neglected the feedback of both the magnetic and electric field onto the fast electron current. Though the laser-generated electrons usually have a Maxwellian distribution [31,36,37], the effect of the velocity dispersion of the fast electrons on the generation of the magnetic field could be negligible here. It is due to the fact that the fast electron current is characterized by the average velocity of the fast electrons, i.e., the fast electrons having energies around the mean energy would have a dominant contribution to the electron current. Contributions from the electrons with energies far away from the mean energy are very small. In addition, both the depth of the buried layer and the thickness of the solid target here are much smaller than the propagation distance of the fast electrons during the laser pulse.

In Figure 2, we show the distribution of the total magnetic field (a), magnetic force term contribution (b), resistive magnetic field (c), and the thermoelectric source term (d), as presented in equation (4). It can be seen that the magnetic field can exceed –5000 T at the front surface of the Cu layer, which is significantly greater than the field generated around the periphery of the fast electron beam due to the resistivity gradient generated by the temperature variation of the target. The contributions of the magnetic force term and thermoelectric source term are very weak compared to the resistive field, and can be ignored, consistently with the above discussion. The term magnetic field refers to the total magnetic field hereafter. Strong resistive magnetic fields generated at the interface of different materials have been observed in recent collisional PIC simulations [38,39], which have a similar magnetic field distribution and magnitude as our results. The Larmor radius of the fast electrons in the magnetic field region would become very small as the magnetic field is large. Then the fast electrons will be magnetized and unable to propagate out of the magnetic field region. Since our concern is whether the fast electrons can propagate through the magnetic field region, the magnetic flux $\phi = \int B dz$ across the interface is the crucial factor affecting fast electron propagation. It is noted that if the magnetic diffusivity is small, the flux will be concentrated as a large magnetic field close to the interface; in the opposite case, the magnetic field will be smaller but spread over a larger distance in z. In other words, the magnetic flux may be similar in both these cases. In order to investigate the magnetic field influence, we will apply the "magnetization

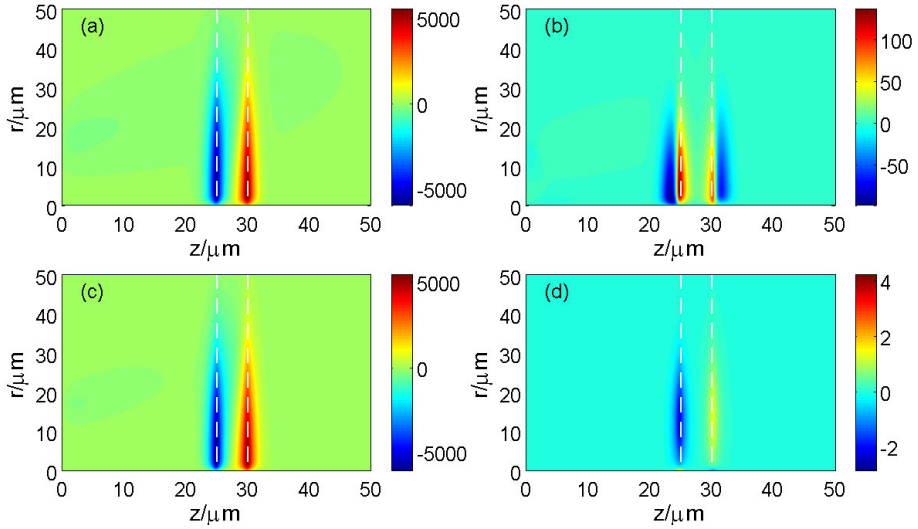

Fig. 2. The distribution of total self-generated magnetic field (a), magnetic force term contribution (b), resistive magnetic field (c), and thermoelectric source term (d) for the case with a laser intensity of $I = 10^{19}$ W/cm^2 and fast electron divergence of 30° at $t = 0.5$ ps. The magnetic field is in units of T and the white dashed lines mark the initial position of the buried layer.

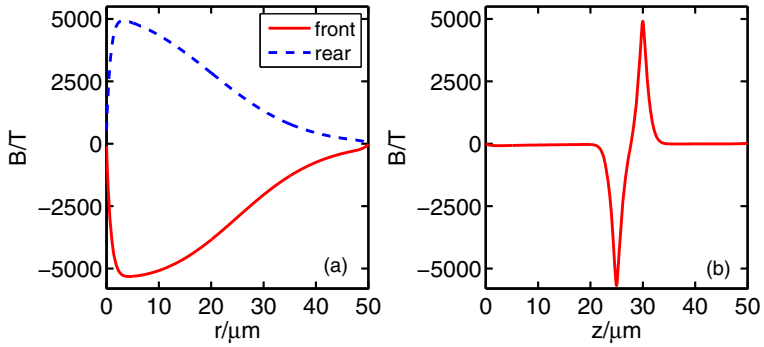

Fig. 3. The distribution of the self-generated magnetic field along the front and rear surface of the buried layer (a) and the magnetic field distribution along the z-axis around $r = 10$ μm (b).

parameter" M suggested by Bell et al. [16] to estimate the magnetic influence at the interface,

$$M = \frac{\int Bdz}{r_L B_c}, \tag{10}$$

where $r_L = \gamma m_e v/eB_c = \sqrt{\gamma m_e k_B T_h}/eB_c$ is the fast electron Larmor radius in the characteristic magnetic field B_c at the interface, $\gamma = (1 - v^2/c^2)^{-1/2}$ is the relativistic factor of the fast electrons. If $M > 1$, the region occupied by the magnetic field is wider than the fast electron Larmor radius and the fast electrons are magnetized. On the contrary, $M < 1$ indicates that the fast electron Larmor radius is large enough to take them outside the magnetic field region, thus they can not be magnetized.

Figure 3 shows the magnetic field profile both at the front and rear surface of the Cu layer. The magnetic field profile along the z-axis is also presented. It can be seen that the profile of the magnetic field at the rear surface is similar to that at the front surface- a little weaker than the latter because of the decrease of the fast electron current density. We have estimated the value of M using the magnetic field given in Figure 3b, which shows that M reaches 3.3, indicating that most of the fast electrons can be magnetized around the interface. This leads to the fast electrons propagating along the interface and ionizing the buried layer, so that the spot size of the K_α X-rays measured in experiments may be wider compared to the case without the buried layer. That is, the measured divergence of the fast electrons may be larger than the intrinsic divergence.

To see the effect of laser pulse duration on the fast electron propagation, the magnetic field distributions along the z-axis for three pulses with different duration are shown in Figure 4. One can see that both of the amplitude and the occupied region of the magnetic field increase with the pulse duration. The value of M can reach 5.2 for the case with a pulse duration of 1 ps, indicating that the fast electron divergence measured in experiments may increase with pulse duration under this condition due to the fact that more and more electrons are confined in the magnetic field region and propagate along the interface.

For comparison, we also vary the buried depth of the Cu layer in the target. Figure 5a shows the magnetic field profile for the cases with three different depths. It can be

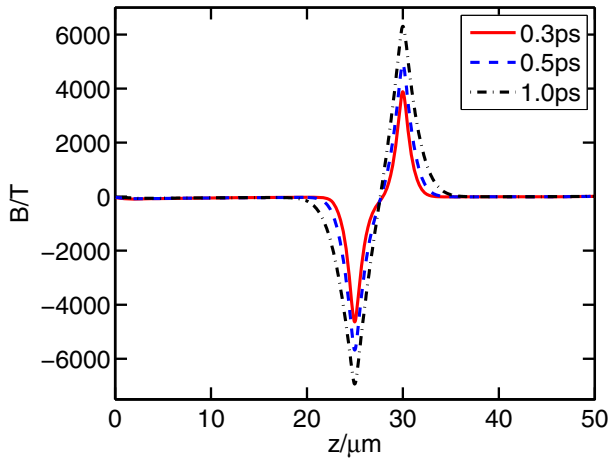

Fig. 4. The evolution of the self-generated magnetic field distribution along the z-axis around $r = 10$ μm.

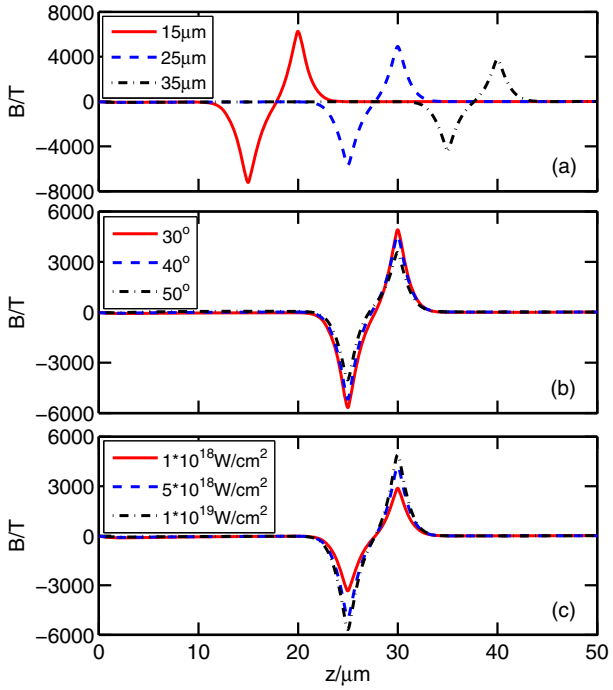

Fig. 5. The profile of the self-generated magnetic field along the z-axis around $r = 10$ μm for the cases with different buried depth (a), different fast electron divergence (b), and different laser intensity (c). The laser intensity is fixed to 10^{19} W/cm^2 in (a) and (b), the fast electron divergence is fixed to 30° in (a) and (c), the depth of the buried layer is fixed to 25 μm in (b) and (c) (same in Fig. 6).

seen that magnetic field decreases with the buried depth due to gradual decrease of the current density through the target. The resistive magnetic field having a form of $\nabla\eta \times \mathbf{j}_h + \eta\nabla \times \mathbf{j}_h$ is the dominant mechanism for the generation of the magnetic field here. Since the gradient of the resistivity is mainly along z-axis, if a fast electron current has a large component in the transverse direction, the first term above should generate a strong magnetic field. This implies that the self-generated magnetic field may be much stronger for a fast electron current with a large divergence. However, in Figure 5b, it is seen that both the magnetic field amplitude and the extent of the region containing the magnetic field decrease with divergence. This is mainly due to the fact that, due to the large divergence, the fast electron current density decreases rapidly as the penetration depth increases. For the higher laser intensity, a larger fast electron current is produced, leading to a stronger magnetic field, as shown in Figure 5c.

For completeness, the magnetization parameters for the cases shown in Figure 5 are estimated, as shown in Figure 6. It can be seen that M decreases with increasing the buried depth of the Cu layer, divergence of the fast electrons and the laser intensity. For all of the cases considered here, M is always greater than 1, indicating that fast electron magnetization occurs. Since the fast electron divergence usually increases with laser intensity [14], in principle larger divergence should be applied for higher laser intensities. That is, the magnetic field effect on the fast electron propagation may be weaker than estimated in Figure 6c for higher laser intensities, but should be taken into account for the cases with a moderate laser intensity. In addition, in order to obtain an accurate measurement of the divergence for the fast electron beam in the experiments, it is generally better to bury the tracer layer farther into the target away from the source of the fast electrons. The magnetic field at the interface in this case would be weaker due to the lower fast electron current in this way.

From the above results, we see that a very strong magnetic field is generated at the interface between the Cu layer and the CH_2 substrate due to the steep resistivity and density gradients between these two materials. The magnetic field amplitude is reduced if one employs a tracer layer with lower Z (e.g. Al) or different combinations such as a Fe target and a Cu tracer layer where the gradients in density and resistivity are less significant. Moreover, to employ a tracer layer with a thickness as small as possible is also beneficial for reducing the magnetic field effects. Figure 7 shows the distribution of the self-generated magnetic field along z-axis for different targets and tracer layers. It can be seen that, since a very thin Cu layer (1 μm) is employed, the magnetic field reduces significantly even for the CH_2 target due to the fact that the magnetic fields at the front and rear surface of the buried layer can counteract each other because of their different polarity and the very thin Cu layer. The magnetization parameter M ($\sim$1.3) is just slightly greater than 1 in this situation. The magnetization parameter is less than 1 for the Al tracer layer, thus the magnetic field influence can be ignored in this case. For the case of Fe target and Cu tracer layer, M is safely below 1 due to that the density and resistivity being very close for these elements. It also can be seen that a strong resistive magnetic field (in the front of the Cu layer and with an amplitude of $\sim$1500 T) is generated around the periphery of the fast electron beam, which can collimate the fast electron beam. This points to the advantage of using thin tracer layers where possible, compatibly with the requirement of generating enough K_α signal to enable

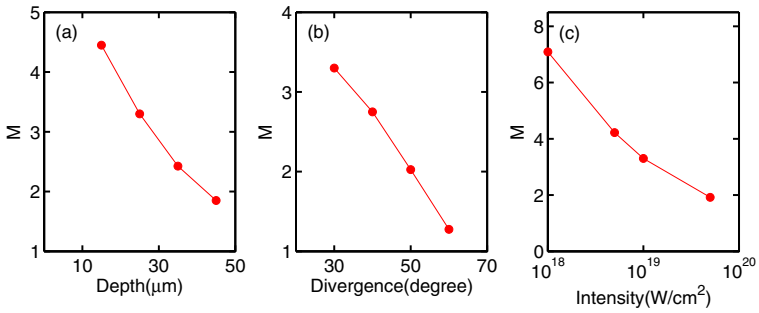

Fig. 6. The magnetization parameter as a function of the depth of the buried layer (a), fast electron divergence (b), and laser intensity (c).

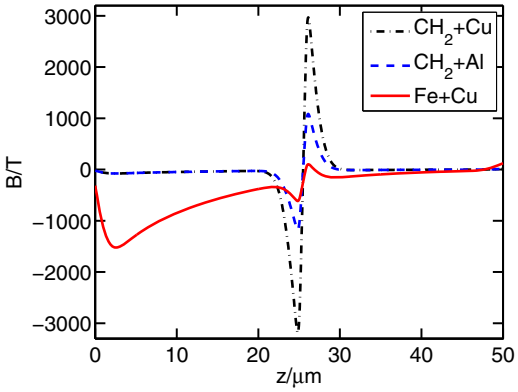

Fig. 7. The profile of the self-generated magnetic field along the z-axis around $r = 10$ μm for the cases with CH_2 target and Cu/Al buried layers and Fe target and Cu buried layer. The thickness of the buried layer is fixed to 1 μm. Other parameters are the same as that in Figure 1.

its detection. Sub-micron layers have indeed been used successfully in experiments diagnosing hot electron propagation, e.g. 0.4–0.5 μm of Al or Cu in references [40,41], and provide a better framework to measure electron propagation with a lower level of magnetic field interference. Reducing significantly the layer thickness below these values is however likely to be unpractical from the point of view of signal strength.

4 Conclusion

In conclusion, the effect of buried layer on the fast electron propagation in a solid target is studied, in conditions of relevance to K_α X-ray emission diagnosis of fast electron divergence. The self-generated magnetic field is derived on the assumption that the cold return current can neutralize completely the fast electron current. Then the magnetic field was solved numerically using a rigid beam model. It is found that the magnetic field generated at the interface between the high-Z layer and the bulk of the target can magnetize the fast electrons and induce fast electrons spread along the interface. This effect becomes weaker as one increases the depth of the tracer layer, the fast electron divergence, and the laser intensity, which indicates that such effect on the fast electron divergence measured from the K_α X-ray emission may need to be considered for the cases with moderate laser intensities as it may alter the fast electron divergence. Utilizing a moderate Z tracer layer or some nearby elements for the tracer layer and bulk target and a thin tracer layer can mitigate the influence of the tracer layer on the fast electron propagation.

We note that our simple calculations can show whether the self-generated magnetic field at the interface will have an effect on the fast electron divergence measured from K_α X-ray emission under certain conditions, but we can not show how large such effect will be. A fully kinetic simulation that includes relativistic collisions of particles is needed to resolve the magnetic field self-consistently due to the steep gradients of the density and resistivity at the interface. This will be the object of future investigations.

This work was supported by NSFC (Grants Nos. 11305264, 11275269, 11175253, and 11375265), RFDP (Grant No. 20114307110020), the Open Fund of the State Key Laboratory of High Field Laser Physics at SIOM, and the Research Program of NUDT. M.B. acknowledges funding from projects ELI (Grant No. CZ.1.05/1.1.00/483/02.0061) and OPVK 3 (Grant No. CZ.1.07/2.3.00/20.0279). X.H.Y. also acknowledges the support from the China Scholarship Council, the Innovation Foundation for Postgraduate of Hunan Province (Grant No. CX2010B008) and NUDT (Grant No. B100204). The authors wish to acknowledge discussions with Dr. D. Riley (QUB).

References

1. M.E. Glinsky, Phys. Plasmas **2**, 2796 (1995)
2. B. Westover, C.D. Chen, P.K. Patel, M.H. Key, H. McLean, R. Stephens, F.N. Beg, Phys. Plasmas **18**, 063101 (2011)
3. X.H. Yang, H. Xu, Y.Y. Ma, F.Q. Shao, Y. Yin, H.B. Zhuo, M.Y. Yu, C.L. Tian, Phys. Plasmas **18**, 023109 (2011)
4. F. Pérez, A. Debayle, J. Honrubia, M. Koenig, D. Batani, S.D. Baton, F.N. Beg, C. Benedetti, E. Brambrink, S. Chawla, F. Dorchies, C. Fourment, M. Galimberti, L.A. Gizzi, L. Gremillet, R. Heathcote, D.P. Higginson, S. Hulin, R. Jafer, P. Koester, L. Labate, K.L. Lancaster, A.J. MacKinnon, A.G. MacPhee, W. Nazarov, P. Nicolai, J. Pasley, R. Ramis, M. Richetta, J.J. Santos, A. Sgattoni, C. Spindloe, B. Vauzour, T. Vinci, L. Volpe, Phys. Rev. Lett. **107**, 065004 (2011)

5. C.R.D. Brown, D.J. Hoarty, S.F. James, D. Swatton, S.J. Hughes, J.W. Morton, T.M. Guymer, M.P. Hill, D.A. Chapman, J.E. Andrew, A.J. Comley, R. Shepherd, J. Dunn, H. Chen, M. Schneider, G. Brown, P. Beiersdorfer, J. Emig, Phys. Rev. Lett. **106**, 185003 (2011)
6. A.B. Sefkow, G.R. Bennett, M. Geissel, M. Schollmeier, B.C. Franke, B.W. Atherton, Phys. Rev. Lett. **106**, 235002 (2011)
7. A. Compant La Fontaine, C. Courtois, E. Lefebvre, Phys. Plasmas **19**, 023104 (2012)
8. M. Borghesi, J. Fuchs, S.V. Bulanov, A.J. MacKinnon, P.K. Patel, M. Roth, Fusion Sci. Technol. **49**, 412 (2006)
9. M. Tabak, J. Hammer, M.E. Glinsky, W.L. Kruer, S.C. Wilks, J. Woodworth, E.M. Campbell, M.D. Perry, R.J. Mason, Phys. Plasmas **1**, 1626 (1994)
10. R.B. Stephens, R.A. Snavely, Y. Aglitskiy, F. Amiranoff, C. Andersen, D. Batani, S.D. Baton, T. Cowan, R.R. Freeman, T. Hall, S.P. Hatchett, J.M. Hill, M.H. Key, J.A. King, J.A. Koch, M. Koenig, A.J. MacKinnon, K.L. Lancaster, E. Martinolli, P. Norreys, E. Perelli-Cippo, M. Rabec Le Gloahec, C. Rousseaux, J.J. Santos, F. Scianitti, Phys. Rev. E **69**, 066414 (2004)
11. K.L. Lancaster, J.S. Green, D.S. Hey, K.U. Akli, J.R. Davies, R.J. Clarke, R.R. Freeman, H. Habara, M.H. Key, R. Kodama, K. Krushelnick, C.D. Murphy, M. Nakatsutsumi, P. Simpson, R. Stephens, C. Stoeckl, T. Yabuuchi, M. Zepf, P.A. Norreys, Phys. Rev. Lett. **98**, 125002 (2007)
12. J.J. Santos, F. Amiranoff, S.D. Baton, L. Gremillet, M. Koenig, E. Martinolli, M. Rabec Le Gloahec, C. Rousseaux, D. Batani, A. Bernardinello, G. Greison, T. Hall, Phys. Rev. Lett. **89**, 025001 (2002)
13. X.H. Yuan, A.P.L. Robinson, M.N. Quinn, D.C. Carroll, M. Borghesi, R.J. Clarke, R.G. Evans, J. Fuchs, P. Gallegos, L. Lancia, D. Neely, K. Quinn, L. Romagnani, G. Sarri, P.A. Wilson, P. McKenna, New J. Phys. **12**, 063108 (2010)
14. J.S. Green, V.M. Ovchinnikov, R.G. Evans, K.U. Akli, H. Azechi, F.N. Beg, C. Bellei, R.R. Freeman, H. Habara, R. Heathcote, M.H. Key, J.A. King, K.L. Lancaster, N.C. Lopes, T. Ma, A.J. MacKinnon, K. Markey, A. McPhee, Z. Najmudin, P. Nilson, R. Onofrei, R. Stephens, K. Takeda, K.A. Tanaka, W. Theobald, T. Tanimoto, J. Waugh, L. Van Woerkom, N.C. Woolsey, M. Zepf, J.R. Davies, P.A. Norreys, Phys. Rev. Lett. **100**, 015003 (2008)
15. X.H. Yang, M. Borghesi, B. Qiao, M. Geissler, A.P.L. Robinson, Phys. Plasmas **18**, 093102 (2011)
16. A.R. Bell, J.R. Davies, S.M. Guerin, Phys. Rev. E **58**, 2471 (1998)
17. R.G. Evans, High Energy Density Phys. **2**, 35 (2006)
18. M.S. Wei, J.R. Davies, E.L. Clark, F.N. Beg, A. Gopal, M. Tatarakis, L. Willingale, P. Nilson, A.E. Dangor, P.A. Norreys, M. Zepf, K. Krushelnick, Phys. Plasmas **13**, 123101 (2006)
19. L.A. Gizzi, S. Betti, E. Föster, D. Giulietti, S. Höer, P. Köter, L. Labate, R. Lözsch, A.P.L. Robinson, I. Uschmann, Phys. Rev. ST Accel. Beams **14**, 011301 (2011)
20. H. Alfvén, Phys. Rev. **55**, 425 (1939)
21. P.M. Bellan, *Fundamentals of Plasma Physics* (Cambridge University Press, 2006)
22. A.J. Kemp, B.I. Cohen, L. Divol, Phys. Plasmas **17**, 056702 (2010)
23. A.R. Bell, A.P.L. Robinson, M. Sherlock, R.J. Kingham, W. Rozmus, Plasma Phys. Control. Fusion **48**, R37 (2006)
24. J.R. Davies, A.R. Bell, M.G. Haines, S.M. Guérin, Phys. Rev. E **56**, 7193 (1997)
25. M. Sherlock, Phys. Rev. Lett. **104**, 205004 (2010)
26. Ph. Nicolaï, J.-L. Feugeas, C. Regan, M. Olazabal-Loumé, J. Breil, B. Dubroca, J.-P. Morreeuw, V. Tikhonchuk, Phys. Rev. E **84**, 016402 (2011)
27. L. Spitzer, R. Härm, Phys. Rev. **89**, 977 (1953)
28. J.J. Honrubia, J. Meyer-ter-Vehn, Plasma Phys. Control. Fusion **51**, 014008 (2009)
29. A.J. Kemp, Y. Sentoku, V. Sotnikov, S.C. Wilks, Phys. Rev. Lett. **97**, 235001 (2006)
30. J.R. Davies, Phys. Rev. E **68**, 056404 (2003)
31. S.C. Wilks, W.L. Kruer, M. Tabak, A.B. Langdon, Phys. Rev. Lett. **69**, 1383 (1992)
32. J.S. Green, K.L. Lancaster, K.U. Akli, C.D. Gregory, F.N. Beg, S.N. Chen, D. Clark, R.R. Freeman, S. Hawkes, C. Hernandez-Gomez, H. Habara, R. Heathcote, D.S. Hey, K. Highbarger, M.H. Key, R. Kodama, K. Krushelnick, I. Musgrave, H. Nakamura, M. Nakatsutsumi, N. Patel, R. Stephens, M. Storm, M. Tampo, W. Theobald, L. Van Woerkom, R.L. Weber, M.S. Wei, N.C. Woolsey, P.A. Norreys, Nat. Phys. **3**, 853 (2007)
33. A.A. Solodov, K.S. Anderson, R. Betti, V. Gotcheva, J. Myatt, J.A. Delettrez, S. Skupsky, W. Theobald, C. Stoeckl, Phys. Plasmas **16**, 056309 (2009)
34. F. Pisani, A. Bernardinello, D. Batani, A. Antonicci, E. Martinolli, M. Koenig, L. Gremillet, F. Amiranoff, S. Baton, J. Davies, T. Hall, D. Scott, P. Norreys, A. Djaoui, C. Rousseaux, P. Fews, H. Bandulet, H. Pepin, Phys. Rev. E **62**, R5927 (2000)
35. P.M. Nilson, A.A. Solodov, J.F. Myatt, W. Theobald, P.A. Jaanimagi, L. Gao, C. Stoeckl, R.S. Craxton, J.A. Delettrez, B. Yaakobi, J.D. Zuegel, B.E. Kruschwitz, C. Dorrer, J.H. Kelly, K.U. Akli, P.K. Patel, A.J. MacKinnon, R. Betti, T.C. Sangster, D.D. Meyerhofer, Phys. Plasmas **18**, 056703 (2011)
36. M.H. Key, M.D. Cable, T.E. Cowan, K.G. Estabrook, B.A. Hammel, S.P. Hatchett, E.A. Henry, D.E. Hinkel, J.D. Kilkenny, J.A. Koch, W.L. Kruer, A.B. Langdon, B.F. Lasinski, R.W. Lee, B.J. MacGowan, A. MacKinnon, J.D. Moody, M.J. Moran, A.A. Offenberger, D.M. Pennington, M.D. Perry, T.J. Phillips, T.C. Sangster, M.S. Singh, M.A. Stoyer, M. Tabak, G.L. Tietbohl, M. Tsukamoto, K. Wharton, S.C. Wilks, Phys. Plasmas **5**, 1966 (1998)
37. K.B. Wharton, S.P. Hatchett, S.C. Wilks, M.H. Key, J.D. Moody, V. Yanovsky, A.A. Offenberger, B.A. Hammel, M.D. Perry, C. Joshi, Phys. Rev. Lett. **81**, 822 (1998)
38. H.B. Zhuo, X.H. Yang, C.T. Zhou, Y.Y. Ma, X.H. Li, M.Y. Yu, Phys. Plasmas **20**, 093103 (2013)
39. S. Chawla, M.S. Wei, R. Mishra, K.U. Akli, C.D. Chen, H.S. McLean, A. Morace, P.K. Patel, H. Sawada, Y. Sentoku, R.B. Stephens, F.N. Beg, Phys. Rev. Lett. **110**, 025001 (2013)
40. S.N. Chen, P.K. Patel, H.K. Chung, A.J. Kemp, S. Le Pape, B.R. Maddox, S.C. Wilks, R.B. Stephens, F.N. Beg, Phys. Plasmas **16**, 062701 (2009)
41. J.A. Koch, M.H. Key, R.R. Freeman, S.P. Hatchett, R.W. Lee, D. Pennington, R.B. Stephens, M. Tabak, Phys. Rev. E **65**, 016410 (2001)